An *IRE*-Like AGC Kinase Gene, *MtIRE*, Has Unique Expression in the Invasion Zone of Developing Root Nodules in *Medicago truncatula*[1][OA]

Catalina I. Pislariu and Rebecca Dickstein*

University of North Texas, Department of Biological Sciences, Denton, Texas 76203–5220

The AGC protein kinase family (cAMP-dependent protein kinases A, cGMP-dependent protein kinases G, and phospholipid-dependent protein kinases C) have important roles regulating growth and development in animals and fungi. They are activated via lipid second messengers by 3-phosphoinositide-dependent protein kinase coupling lipid signals to phosphorylation of the AGC kinases. These phosphorylate downstream signal transduction protein targets. AGC kinases are becoming better studied in plants, especially in Arabidopsis (*Arabidopsis thaliana*), where specific AGC kinases have been shown to have key roles in regulating growth signal pathways. We report here the isolation and characterization of the first AGC kinase gene identified in *Medicago truncatula*, *MtIRE*. It was cloned by homology with the Arabidopsis *INCOMPLETE ROOT HAIR ELONGATION* (*IRE*) gene. Semiquantitative reverse transcription-polymerase chain reaction analysis shows that, unlike its Arabidopsis counterpart, *MtIRE* is not expressed in uninoculated roots, but is expressed in root systems that have been inoculated with *Sinorhizobium meliloti* and are developing root nodules. *MtIRE* expression is also found in flowers. Expression analysis of a time course of nodule development and of nodulating root systems of many *Medicago* nodulation mutants shows *MtIRE* expression correlates with infected cell maturation during nodule development. During the course of these experiments, nine *Medicago* nodulation mutants, including *sli* and *dnf1* to *7* mutants, were evaluated for the first time for their microscopic nodule phenotype using *S. meliloti* constitutively expressing *lacZ*. Spatial localization of a p*MtIRE-gusA* transgene in transformed roots of composite plants showed that *MtIRE* expression is confined to the proximal part of the invasion zone, zone II, found in indeterminate nodules. This suggests *MtIRE* is useful as an expression marker for this region of the invasion zone.

Nitrogen-fixing root nodules are the result of a complex and unique interaction between leguminous plants and soil rhizobia. During nodule development, rhizobia are brought into roots through infection threads that originate in deformed root hairs that curl to form a so-called ''shepherd's crook.'' Infection thread initiation and growth require living rhizobia that are synthesizing specific Nod factors (Ardourel et al., 1994; Limpens et al., 2003). Infection threads bring rhizobia past several root cell layers and deposit them into newly divided nodule cells within a membrane-bounded compartment called the symbiosome in a process resembling endocytosis. Within the infected cells, an environment is established where the rhizobia and plant express new proteins that enable biochemical support of nitrogen fixation and assimilation. In indeterminate nodulators such as *Medicago truncatula*, new infections occur continuously over the lifetime of the nodule, with new infections starting below the meristematic distal end of the nodule at the beginning of the infection zone, zone II. In the proximal end of zone II, both rhizobia and plant cells expand and mature. Exit from zone II is marked by starch accumulation, which the rhizobia apparently use as a carbon source as they continue their maturation to nitrogen fixation capability in zone III (Vasse et al., 1990). Reviews on legume root nodule development are available (Brewin, 1991; Kijne, 1992; Gage and Margolin, 2000; Brewin, 2004; Gage, 2004).

Nodule-specific (nodulin) and nodule-enhanced genes are expressed exclusively and primarily in nodules, respectively. Most nodulin genes have homologs in nonlegumes, suggesting that nodule-specific genes have been recruited from other developmental pathways. It has been noted that a number of nodulins are also expressed in nonsymbiotic tissue, including in floral tissues (Szczyglowski and Amyot, 2003). In some cases, genes expressed in both nodules and in floral tissue may have a role in tip growth during infection thread and pollen tube growth, respectively (Rodriguez-Llorente et al., 2004). Other tissues with tip growth, a type of cell expansion, include root hair cells, which have been used as a model system to study tip growth, especially in Arabidopsis (*Arabidopsis thaliana*; Schiefelbein, 2000).

The AGC protein kinases contain the protein kinase A, protein kinase G, and protein kinase C regulatory kinases. In animals and fungi, members of this kinase

[1] This work was supported by the National Science Foundation (IOB no. 0520728) and by the University of North Texas (faculty research funds to R.D.).

* Corresponding author; e-mail beccad@unt.edu; fax 940–565–3821.

The author responsible for distribution of materials integral to the findings presented in this article in accordance with the policy described in the Instructions for Authors (www.plantphysiol.org) is: Rebecca Dickstein (beccad@unt.edu).

[OA] Open Access articles can be viewed online without a subscription.

www.plantphysiol.org/cgi/doi/10.1104/pp.106.092494

family act in protein phosphorylation cascades. In animals, a key AGC kinase regulator is the 3-phosphoinositide-dependent protein kinase (PDK1), a central growth regulator that integrates signaling events from receptors that stimulate the synthesis of phosphatidylinositol 3,4,5-trisphosphate (Bogre et al., 2003; Mora et al., 2004). Far less is known about AGC kinases in plants. In Arabidopsis, at least 39 AGC kinase genes have been identified (Bogre et al., 2003), but only seven have known functions. *INCOMPLETE ROOT HAIR ELONGATION* (*IRE*; referred to as *AtIRE* here) controls the duration of root hair growth in Arabidopsis (Oyama et al., 2002). *AGC2-1/OXI1* also regulates root hair development (Anthony et al., 2004; Rentel et al., 2004) and mediates stress signaling (Rentel et al., 2004; Anthony et al., 2006). *PINOID* plays a role in asymmetrical localization of membrane proteins during polar auxin transport (Christensen et al., 2000). Phototropins 1 and 2 (*PHOT1* and *PHOT2*) mediate blue light signaling (Huala et al., 1997; Briggs and Christie, 2002; Takemiya et al., 2005). *ADI3* and *PDK1* both regulate plant cell death (Devarenne et al., 2006). The Arabidopsis AGC kinases group phylogenetically into five subfamilies (Bogre et al., 2003). A sixth subfamily, called AGC Other according to the Hanks classification (Hanks and Hunter, 1995), contains *AtIRE* and homologous *IRE* genes.

The *Medicago* genome project has identified many potential genes with roles in nodule development by virtue of their being found as expressed tag sequences (ESTs) only in cDNA libraries prepared from tissue that includes nodules (Fedorova et al., 2002; El Yahyaoui et al., 2004; Lohar et al., 2006). One of the genes identified in this manner is *MtIRE*, a *Medicago* homolog of the *AtIRE* gene. In this work, we present results showing the cloning of the complete *MtIRE* cDNA and its relationship to *AtIRE* and *IRE*-like genes. We investigate *MtIRE* expression in plant tissues during nodule development and in symbiotically defective *Medicago* mutants. Our findings show that *MtIRE* does not have a role in root hair growth in *Medicago* and suggest the role of *MtIRE* is likely to be in maturation of infected nodule cells in zone II, before effective symbiotic nitrogen fixation occurs.

RESULTS

Isolation and Sequence of the Complete *MtIRE* Gene

In 2002, Fedorova et al. reported 340 tentative consensus (TC) sequences comprising ESTs found only in cDNA libraries that were made from *M. truncatula* nodule-containing tissue (Fedorova et al., 2002). One of these was TC33166, currently annotated as TC103185 in The Institute for Genomic Research MtGI 8.0 release (www.tigr.org). TC103185, 1,383 nucleotides long, consists of four ESTs; its strongest BLASTX hit is the Arabidopsis *AtIRE* protein kinase-like gene (GenBank accession no. AB037133; Oyama et al., 2002). Using the working draft of overlapping bacterial artificial chromosome (BAC) clones mth2-13b8 and mth1-8d23 (GenBank accession nos. AC122727 and AC133139, respectively) containing the genomic copy of TC103185, sequence from TC103185, and the *AtIRE* gene, primers were chosen to reverse transcribe and amplify *M. truncatula* A17 nodule mRNA corresponding to *MtIRE* of progressively increasing sizes. These efforts resulted in a cDNA containing the complete *MtIRE* coding region of 3,504 nucleotides. Subsequently, 5′- and 3′-RACE were carried out to identify the 5′ and 3′ ends of the *MtIRE* transcript. 5′ RACE identified three different 5′ ends corresponding to untranslated 5′ regions of 174, 120, and 115 bases upstream of the predicted translational start codon. 3′-RACE yielded a single 3′ end that contained 296 nucleotides 3′ to the predicted translational stop. The complete *MtIRE* cDNA of 3,974 nucleotides corresponding to the longest transcript detected is available in the GenBank database (accession no. AY770392).

Characterization of *MtIRE* Gene Structure and Its Encoded Protein

The *Medicago* genome project has mapped BACs mth2-13b8 and mth1-8d23 containing *MtIRE* to chromosome 5 (www.medicago.org/genome). Comparison of the *MtIRE* genomic and cDNAs revealed that the *MtIRE* gene spans a genomic region of 9.1 kb and consists of 17 exons and 16 introns (Fig. 1A). This organization is almost identical to the *AtIRE* gene, which is shown for comparison in Figure 1B. Both genes have 17 exons of similar sizes, but in the *Medicago MtIRE* gene the introns are significantly larger than in the *AtIRE* gene. The Arabidopsis genome has four other *IRE*-like genes. Their genome organization is similar to *AtIRE* and to *MtIRE* although slight differences are noted, especially extra exons in *AtIRE_2* and the lack of the first three exons in *AtIRE_3* (Fig. 1C).

The third start codon (ATG) from the 5′ end of the transcript is the presumed start site for the longest open reading frame of the *MtIRE* gene. *MtIRE* encodes a deduced protein of 1,168 amino acid residues. ExPASy (www.expasy.org/tools/scanprosite; Gattiker et al., 2002) and BLAST (www.ncbi.nlm.nih.gov/BLAST/; Altschul et al., 1990) tools were used to analyze the deduced *MtIRE* protein (Fig. 1D). It contains a Glu-rich region at its N-terminal end, basic-type (Kalderon et al., 1984) and bipartite-type (Robbins et al., 1991) nuclear localization signals, a zinc finger-like sequence (C-X_2-C-X_{11}-H-X_3-C; Fig. 1D; Bohm et al., 1997), and numerous potential phosphorylation sites, including those for casein kinase II, protein kinase C, cAMP-, cGMP-, and phosphoinositide-dependent protein kinases. *MtIRE* contains a putative Ser/Thr protein kinase domain toward its C-terminal end (Fig. 1D). Within the Ser/Thr protein kinase domain is an activation loop motif that is a putative target of PDK1. C terminal to the kinase domain is the PDK1-interacting fragment (PIF) found in some PDK1 substrates (Fig. 1D). Both the

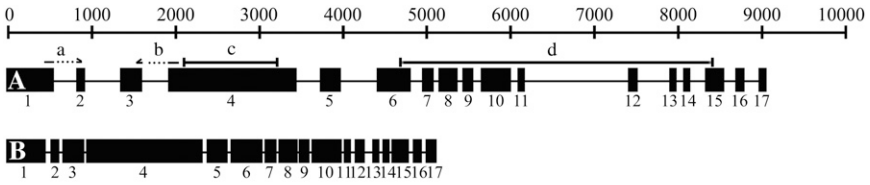

C

Gene \ Exon	a	b	1	2	3	4	5	6	7	8	9	10	11	12	13	14	15	16	17
MtIRE			451	65	174	1263	173	250	95	141	91	204	84	89	52	57	162	81	72
AtIRE			424	68	177	1257	173	250	93	141	93	205	86	89	52	57	156	84	99
AtIRE_H1			715	66	183	1353	173	243	93	141	93	205	86	89	52	57	177	78	87
AtIRE_2	98	723	103	65	183	1353	173	244	93	141	93	205	86	89	52	57	97	155	87
AtIRE_3						1095	173	232	93	141	93	187	86	89	52	57	174	78	87
AtIRE_4			205	101	177	1215	173	226	93	141	93	193	86	89	52	57	129	75	99

D

```
MSSNPPPPENDPPPATSSPVSAKSRTLQKFPPIVNRRTATLSSNNVDDECKEENNKNKNH      60
DNEEESEEEEEEEEEEEEDVLVTEREFERAECSYSSSILQASSLGLNQIRTRFSSPLRHS     120
SSAGAPSFPIKDVVNNVAKFRSRVSHPKDLGEKVHWMQSKSLKARSQLLILEGNHAAYAK     180
DFQSPRYQEILRLTSGKKRKNRPDIKSFSHELNSKGVRPFPVWKNRAFGQEIMEEIRAKF     240
EKLKEEVDSDLGGFAGDLVGTLEKIPGSHPEWKEGLEDLLVVARQCAKMTAAEFWINCET     300
IVQKLDDKRQDIPVGILKQAHTRLLFILSRCTRLVQFQKESVKEQDHILGLHQLSDLGVY     360
SEQIMKAEESCGFPPSDHEMAEKLIKKSHGKEQDKPITKQSQADQHASVVIDNVEVTTAS     420
TDSTPGSSYKMASWRKLPSAAEKNRVGQDAVKDENAENWDTLSCHPDQHSQPSSRTRRPS     480
WGYWGDQQNLLHDDSMICRICEVEIPILHVEEHSRICTIADKCDLKGLTVNERLERVAET     540
IEMLLDSLTPTSSLHEEFNELSLERNNMSSRCSEDMLDLAPDNTFVADDLNLSREISCEA     600
HSLKPDHGAKISSPESLTPRSPLITPRTSQIEMLLSVSGRRPISELESYDQINKLVEIAR     660
AVANANSCDESAFQDIVDCVEDLRCVIQNRKEDALIVDTFGRRIEKLLQEKYLTLCEQIH     720
DERAESSNSMADEESSVDDDTIRSLRASPINGFSKDRTSIEDFEIIKPISRGAFGRVFLA     780
QKRSTGDLFAIKVLKKADMIRKNAVEGILAERDILISVRNPFVVRFYYSETCKENLYLVM     840
EYLNGGDLYSMLRNLGCLDEDMARVYIAEVVLALEYLHSQSIVHRDLKPDNLLIGQDGHI     900
KLTDFGLSKVGLINSTEDLSAPASFTNGFLVDDEPKPRHVSKREARQQQSIVGTPDYLAP     960
EILLGMGHGTTADWWSVGVILYELLVGIPPFNADHAQQIFDNIINRDIQWPKHPEEISFE    1020
AYDLMNKLLIENPVQRLGVTGATEVKRHAFFKDVNWDTLARQKAMFIPSAEAHDTSYFMS    1080
RYIWNVEDDEHCAGGSDFYDHSETSSSGSGSDSLDEDGDECASLTEFGNSALGVQYSFSN    1140
FSFKNISQLVSINMMHISKETPDDSNPS                                    1168
```

activation loop motif and the PIF are signature sequences of the AGC family (Bogre et al., 2003; Mora et al., 2004).

Relationship with Other *IRE* and AGC Protein Kinase Genes

BLAST (Altschul et al., 1990) was used to search for *MtIRE* homologs in the Arabidopsis, rice (*Oryza sativa*), and tomato (*Lycopersicon esculentum*) genomes, as well as the unfinished *Medicago* genome (Young et al., 2005). In the *Medicago* genome, 20 other ESTs or TCs (www.tigr.org) were found that had homology to AGC protein kinases (Table I). Unfortunately, none of these represents a complete cDNA; many contain a recognizable full or partial Ser/Thr protein kinase domain. Of these, three were found by BLAST or ClustalW (Thompson et al., 1994) to be *IRE*-like ESTs or TCs that belong to the AGC Other subfamily of AGC genes (Bogre et al., 2003). The other 17 were more similar to different AGC protein kinases than to the *IRE*/AGC Other family (data not shown).

MtIRE, *IRE* homologs, and the Arabidopsis AGC kinases (Bogre et al., 2003) were subjected to phylogenetic analysis using ClustalW (Thompson et al., 1994) and the neighbor-joining method. The *Medicago IRE* genes were found to group as a single clade with the *AtIRE*, rice *OsIRE*, and tomato *LeIRE* genes (Fig. 2). This suggests that *MtIRE*, *AtIRE*, and other *IRE*-like genes diverged from the other AGC kinases before the monocots and dicots diverged, estimated to be about 170 million years ago (Sanderson et al., 2004). *MtIRE* was found to form a subclade with *AtIRE* within the *IRE* clade (Fig. 2), suggesting that these two genes are orthologous.

The N termini of *MtIRE*, *AtIRE*, and *OsIRE* are highly diverged (not shown), while the putative nuclear localization sequences, zinc finger, PIF motif, and Ser/Thr protein kinase domain are conserved (Fig. 3). Within the Ser/Thr protein kinase domain, the activation loop signature motif is conserved among the *IRE* genes, including *MtIRE*. However, the putative PDK1 kinase target Ser residue of the activation loop was found to be missing in both *AtIRE* and *OsIRE*; it is

Figure 1. *MtIRE* genomic organization and coding region. A and B, The *MtIRE*-deduced exons (black boxes) and introns (lines; A) are compared to those of *AtIRE* (B). A, Arrows a and b show positions of primers used for RT-PCR; lines c and d show the positions of the exon 4 cDNA probe and the Ser/Thr kinase domain cDNA probe used for Southern blots. C, Comparison of the *MtIRE* exons to those of all the Arabidopsis *IRE* genes. D, Deduced *MtIRE* amino acid sequence. Dotted underline, Glu-rich region; boxed shaded type, basic nuclear localization signal; single underline, zinc finger; double underline, bipartite nuclear localization signal; bold type, Ser/Thr protein kinase domain; boxed bold type, activation loop signature; asterisk, Ser residue in activation loop that is putative phosphorylation target; double dotted underline, PIF motif.

Table I. *Medicago AGC kinase ESTs and TCs*

Medicago EST/TC	Closest Arabidopsis Homolog(s)	Closest Homolog(s), Other Plants
TC97389	AtIRE	OsIRE4 (rice)
BF643568	AtIRE_H1	
AW774942	AtIRE_3	LeIRE (tomato)
TC101401	AtNDR1, AtNDR3	*Medicago* TC101402
TC101402	AtNDR1, AtNDR3	*Medicago* TC101401
TC101475	AtNDR6	
TC95471	AtNDR8	
TC98351	AtPHOT1, AtPHOT2	*Medicago* TC97767
TC97767	AtPHOT1, AtPHOT2	*Medicago* TC98351
TC94584	AtS6K_1	
TC109296	AtAGC1_9, AtKIPK	
TC108869	AtPK7	
TC94569	AtPK5	
TC95276	AtAGC2_3, AtACT2_4	
TC103992	AtACG1_3	
TC110242	AtS6K_1	
TC107335	AtPDK1_1, AtPDK1_2	*Medicago* TC94724, TC94724, TC94899
TC94724	AtPDK1_1, AtPDK1_2	*Medicago* TC107335, TC94659, TC94899
TC94659	AtPDK1_1, AtPDK1_2	*Medicago* TC107335, TC94724, TC94899
TC94899	AtPDK1_1, AtPDK1_2	*Medicago* TC107335, TC94724, TC94659

present in *MtIRE* (Fig. 3D) and also present in the other *IRE* genes for which full sequence is available (not shown).

MtIRE Is a Single Copy Gene in *Medicago*

To experimentally determine the *MtIRE* copy number in *M. truncatula*, Southern-blot analysis was carried out. *M. truncatula* genomic DNA was restricted with several enzymes, blotted, and probed with a cDNA probes derived from exon 4 of *MtIRE* (Fig. 1). The results obtained at low stringency (not shown) are similar to those obtained at high stringency (Fig. 4), showing one or two bands per lane. These results are consistent with *MtIRE* being a single copy gene in *M. truncatula*, and, with the exception of the pattern obtained with *Hin*cII enzyme, consistent with predicted in silico restriction pattern. In some cases, *Hin*cII cleavage is affected by DNA methylation, which may account for the inconsistency with the in silico prediction. Probing the blot with a different cDNA derived from the putative Ser/Thr kinase domain (Fig. 1) yielded similar results of one or two bands per lane, also consistent with *MtIRE* being single copy (not shown).

MtIRE Expression Is in Nodules and Flowers

To examine *MtIRE* expression, semiquantitative reverse transcription (RT)-PCR was carried out on total RNA extracted from different plant tissues of *M. truncatula* A17 wild-type plants. RT-PCR primers were chosen to flank introns (Fig. 1). The transcript of the *MtIRE* gene was detected only in nodules and flowers and not in other organs of the plant, including uninoculated roots (Fig. 5A).

To determine when during nodule development *MtIRE* is first expressed, a time course of *MtIRE* expression in roots with developing nodules was carried out. The results show that *MtIRE* is first expressed at 4 d postinoculation (dpi) of nitrogen-starved roots with *Sinorhizobium meliloti* (Fig. 5B). This is well before the onset of nitrogen fixation in growth conditions used for these experiments, at about 8 dpi.

MtIRE Expression in Nodulating Roots of *M. truncatula* Nodulation Mutants

To further pin down the stage of nodule development with which *MtIRE* gene expression is associated, *M. truncatula* nodulation mutants were examined for *MtIRE* expression in nodulated root systems or root areas susceptible to nodulation 10 dpi after inoculation with *S. meliloti*, also by semiquantitative RT-PCR. As shown in Figure 6A, *MtIRE* was found to be expressed in both supernodulators tested, *sunn* (Penmetsa et al., 2003) and *skl* (Penmetsa and Cook, 1997). Mutants defective in Nod factor signal transduction, like *dmi2* (Catoira et al., 2000), fail to express *MtIRE. MtIRE* gene expression was not detected in nodulated root systems of mutants that have defects in nodule invasion: *lin* (Kuppusamy et al., 2004), *sli* (Haynes et al., 2004), *nip* (Haynes et al., 2004; Veereshlingam et al., 2004), and *Mtsym1* (TE7; Benaben et al., 1995; Fig. 6A). In *lin*, *sli*, and *nip* nodules, almost all nodules contain rhizobia trapped within infection threads, whereas in *Mtsym1* nodules, rhizobia are endocytosed into host cells and undergo limited replication but fail to elongate into bacteroids. *M. truncatula dnf* mutants, *dnf1* to *7* (Mitra and Long, 2004; Starker et al., 2006), deficient in nitrogen fixation, were examined in a similar fashion. In comparison to the mutants blocked very early in nodule development or during rhizobial invasion, all

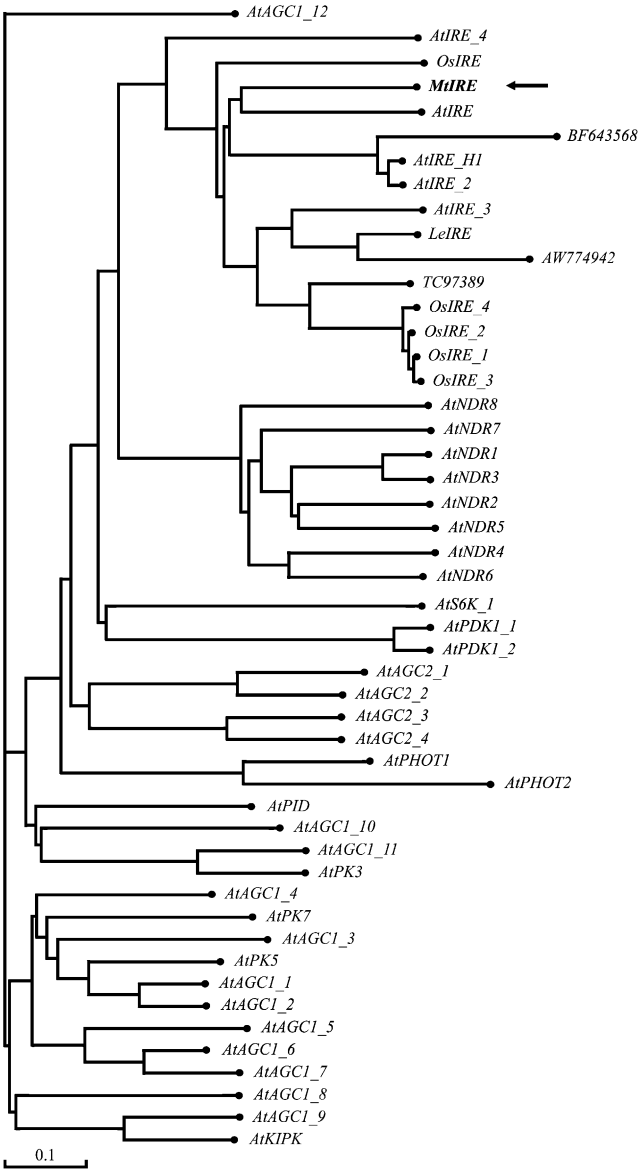

Figure 2. Phylogram of Arabidopsis AGC protein kinases and plant *IRE* and *IRE*-like genes. The amino acid sequences used in the alignment were obtained from the GenBank database. The alignment was conducted using the Clustal method with default options. The abbreviations used are as follows: Mt, *M. truncatula*; At, Arabidopsis; Os, rice; Le, tomato.

of the *dnf* mutants were found to express *MtIRE* (Fig. 6B). However, the level of *MtIRE* expression was found to be lower than in wild type in some of the *dnf* mutants. The *dnf* mutants were grouped into three classes, based on the extent of *MtIRE* expression (Fig. 6B). In the first class are the *dnf1-1*, *dnf1-2*, and *dnf5* mutants that had significantly lower expression of *MtIRE* in their nodulated root systems. The second class contains *dnf7*, which has lower expression of *MtIRE*. The third class includes *dnf2*, *dnf3*, *dnf4*, and *dnf6* mutants that have wild-type levels of *MtIRE* expression in their nodulated root systems.

To correlate *MtIRE* expression in the mutant nodules with phenotypes of the mutants, microscopic analyses of mutant nodules were carried out by examining X-Gal-stained 50-μm sections of nodules or whole roots of mutant plants inoculated with *S. meliloti/hemA::lacZ* (Boivin et al., 1990), also at 10 dpi (Fig. 7). While similar analyses have been reported for some of the mutants used in this study, it was important to verify the phenotypes under the growth conditions employed in these experiments.

As shown in Figure 7A, for the *skl* mutant, more nodules than wild type, all staining so darkly blue they almost look black, were detected, as reported previously (Penmetsa and Cook, 1997). For *dmi2*, no invasion was seen; as reported previously, root hairs developed bulbous tips (Catoira et al., 2000; Fig. 7B). For the four mutants with defects in rhizobial invasion, *lin*, *sli*, *nip*, and *Mtsym1*, a gradient of rhizobial infection was observed, with *lin* infections confined to the root hair cell containing the initial infection thread, similar to published observations (Kuppusamy et al., 2004; Fig. 7C). In the *sli* mutant, infections progressed further, with infection threads penetrating the outer cortical cells and occasionally reaching inner cortical cells (Fig. 7D). The rare invaded nodules seen previously (Haynes et al., 2004) at much later times postinoculation were not observed in our growth conditions at the 10-dpi time point. In the *nip* mutant, infection threads filled nodule primordia that showed signs of defense responses by accumulating brown pigments, as described previously (Veereshlingam et al., 2004; Fig. 7E). For *Mtsym1* (Benaben et al., 1995; Fig. 7F), nodule primordia filled with infection threads were readily observed, as were nodules with rhizobia released into plant cells. Brown pigments were observed, although the accumulation of these pigments was less than in the *nip* mutant and were distributed differently from those in *nip*, mostly around infection threads in *Mtsym1*. These results are similar to those previously described by some researchers (Benaben et al., 1995). The small, uninvaded *Mtsym1* bumps seen by others (Benaben et al., 1995; Mitra and Long, 2004) were only rarely observed in our conditions.

The *dnf* mutants' nodules host cells all showed evidence of released rhizobia around a central vacuole (Fig. 7, G–R). Nodules from the *dnf1* and *dnf5* mutants appeared to have the most serious defects. *dnf1-1* and *dnf1-2* nodules were characterized by large accumulations of brown-orange pigments in the most proximal zone developed in these nodules. To a lesser extent, these pigments also accumulated in the nodule parenchyma (Fig. 7, G and H). In the *dnf5* mutant, the rhizobia occupying infected cells appeared to be sparser than in wild-type nodules, and some accumulation of pigments was observed (Fig. 7N). The *dnf2* mutant nodules appeared to have lower rhizobial occupancy but were clearly invaded by rhizobia. Only a small pale-yellow band that may be polyphenolic accumulation near the invasion zone was noted (Fig. 7I). For the *dnf3*, *dnf4*, *dnf6*, and *dnf7* mutants, at least two

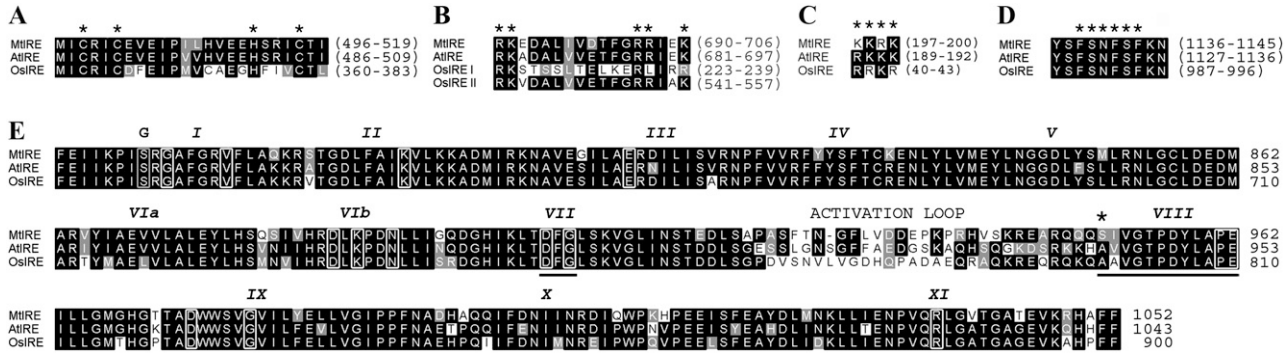

Figure 3. Alignments of conserved domains in the *MtIRE*, *AtIRE*, and *OsIRE* predicted protein sequences. Amino acid residue positions are indicated on the right of each aligned sequence. A, Zinc finger domain. Asterisks show the conserved Cys and His residues. B, Bipartite nuclear targeting sequence. Asterisks show the conserved Arg and Lys residues. Note that OsIRE contains two bipartite nuclear localization signal sequences. C, Basic-type nuclear targeting sequence. Asterisks show basic Arg and Lys residues. D, PIF motif. Asterisks show the conserved amino acid residues of the motif. E, Ser/Thr kinase domain. Roman numerals denote the 12 distinct subdomains, as described in Hanks and Hunter (1995). White-boxed residues are conserved residues found in Ser/Thr kinase domains and the gray-boxed Ser residue in subdomain I is Ser in all three *IRE* sequences, but G in the conserved kinase family (Hanks and Hunter, 1995). The position of the activation loop is noted with the amino acids in the activation loop signature motif (Bogre et al., 2003) underlined.

different phenotype nodules were observed in our growth conditions. One type appeared defective with lower rhizobial occupancy in the infected cells (Fig. 7, J, L, O, and Q), while the second type was hard to distinguish from wild type (Fig. 7, K, M, P, and R). For the case of *dnf7* mutants, nodulated root systems displayed only a few of the wild-type phenotype nodules (as in Fig. 7R). The defective *dnf7* nodules look quite abnormal, with rhizobia accumulating in a band toward the apex of the nodule (Fig. 7Q).

To look more closely at mutant nodules not expressing *MtIRE* versus those with low levels of *MtIRE* expression, higher magnifications were used to compare the phenotypes of the *nip* and *Mtsym1* nodules to those of *dnf1* and *dnf5* (Fig. 8). Both *nip* and *Mtsym1* nodules contain rhizobia mostly confined within infection threads (Fig. 8, A and B). At the subcellular level, both mutants have been shown by electron microscopy to have rhizobial release into host cells; in *nip*, this is a rare event, but it is frequent in *Mtsym1* (Benaben et al., 1995; Veereshlingam et al., 2004). In contrast, the *dnf1-1*, *dnf1-2*, and *dnf5* nodules have host plant cells with released rhizobia around a central vacuole, as in wild type. In the *dnf1* mutants, rhizobia also accumulate as dark blue patches in the intercellular spaces (Fig. 8, C and D). In the *dnf5* nodules, a lower rhizobial occupancy than wild type was observed with rhizobia accumulating in thinner rings around the central vacuole than they do in wild type (Fig. 8, compare E with F). Brown pigmentation indicative of polyphenolic accumulation is evident in the *nip*, *dnf1*, and *dnf5* mutants (Fig. 8, B–E).

Spatial Localization of Nodule *MtIRE* Expression

To examine the spatial localization of *MtIRE* expression, an *MtIRE* promoter-*GUS* reporter construct (p*MtIRE-gusA*) was made and expressed in transgenic roots in composite *M. truncatula* wild-type plants. Plants were inoculated with rhizobia carrying a constitutive *hemA* gene, and nodulated roots were harvested at 15 dpi. Nodules formed asynchronously and more slowly in the composite plants than in untransformed roots, and nodules were found at various stages of development in the composite plants at 15 dpi in our growth conditions. Fixed tissue was stained with 5-bromo-4-chloro-3-indolyl-β-glucuronic acid (X-gluc) to visualize p*MtIRE-gusA*. The largest wild-type nodules were costained with Red-Gal to visualize the rhizobia. The results (Fig. 9A) show that blue staining indicative of *MtIRE* expression is confined to a narrow zone toward the apical end of the mature nodule, with red-staining rhizobia both apical and distal to the X-gluc-staining region. Transgenic nodules from composite plants were also stained with iodide to localize the starch, defining the interzone II-III region of the nodule (Vasse et al., 1990). By comparing the results of iodide staining (Fig. 9B) with that for Red-Gal and X-gluc staining, it can be seen that p*MtIRE-gusA* expression localizes apically to the iodide staining, showing that *MtIRE* expression starts at the proximal end of the infection zone, zone II, but ends before the interzone II-III region. Costaining with X-gluc and iodide confirms that *MtIRE* expression is distal to the iodide staining region (data not shown), demonstrating the *MtIRE* expression is confined to the zone II invasion region of the nodule. As expected, and in confirmation of the semiquantitative RT-PCR expression results, no expression was detected in root hairs, even those containing infection threads (Fig. 9C).

Expression of the p*MtIRE-gusA* construct in composite *dnf1-2* and *dnf7* plants was evaluated to test the validity of using *MtIRE* as a marker for invaded nodule cell tissue. The results showed p*MtIRE-gusA*

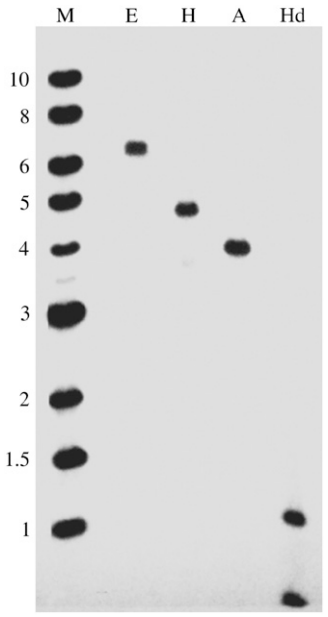

Figure 4. Southern-blot analysis of *M. truncatula* genomic DNA. DNA was restricted with *Eco*RI (E), *Hin*cII (H), *Ase*I (A), or *Hin*dIII (Hd) and subjected to Southern analysis with DNA prepared from exon 4 of *MtIRE*. Markers were run in an adjacent lane and the blot was subsequently probed with DNA prepared from the marker DNA. Sizes of the markers are indicated on the left.

expression in both mutants as expected. *dnf1-2* has smaller nodules than does *dnf7* (and wild type) and p*MtIRE-gusA* staining was confined to the proximal end of the largest *dnf1-2* nodules observed (Fig. 9D). For the largest observed *dnf7* nodules, staining was observed in approximately the nodule middle (Fig. 9E), suggesting that *dnf7* nodules are capable of further development than are those of *dnf1-2*.

A pictorial interpretation of the visualized staining pattern for wild-type nodules is presented in Figure 9F. p*MtIRE-gusA* is confined to the proximal side of zone II, and thus may be a marker for this developmental zone.

DISCUSSION

In 2002, Fedorova et al. reported nodule-specific TC sequences found in *Medicago*. Among these was a TC with high homology for the *AtIRE* gene, with a predicted signal transduction function (Fedorova et al., 2002). Because the *AtIRE* gene has a known role in root hair elongation and is thought to function in regulating the duration of tip growth (Oyama et al., 2002), we thought that the *MtIRE* gene might have a similar role in *Medicago* or one regulating infection thread growth, which can be viewed as inward apical growth, similar to root hair tip or pollen tube growth.

MtIRE is a member of the AGC family of Ser/Thr protein kinases involved in signal transduction. In many animal AGC kinases, activation depends on sequential phosphorylation at two sites, one within the PIF motif, found C terminal to the kinase domain, and one within the activation loop of the kinase domain (Mora et al., 2004). Although well studied in animals, the signaling pathways regulated by AGC kinases in plants are not yet well understood. In Arabidopsis, seven of at least 39 AGC kinases have been partially characterized as having important roles in development (Huala et al., 1997; Christensen et al., 2000; Briggs and Christie, 2002; Oyama et al., 2002; Bogre et al., 2003; Anthony et al., 2004, 2006; Takemiya et al., 2005; Devarenne et al., 2006; Zegzouti et al., 2006), and a number of other AGC kinases are under study (Zegzouti et al., 2006). *MtIRE* is the first AGC kinase studied in legumes.

The large plant AGC kinase family is subdivided into distinct phylogenetic classes (Bogre et al., 2003), with the *IRE* genes, including *MtIRE*, clustering in a single clade (Fig. 2). Of these genes, *AtIRE* and *AtIRE H1* have been previously studied (Oyama et al., 2002). In addition to sequence motifs characteristic of AGC kinases, *MtIRE* encodes a putative zinc finger-like sequence and nuclear localization sequences (Fig. 3). This suggests that *MtIRE* protein, like some of the other *IRE* genes, could localize to the nucleus, similar to the *NDR* proteins of the AGC family that also contain nuclear localization signals (Tamaskovic et al., 2003). Unique to this *IRE*-like gene, *MtIRE* encodes a Glu-rich sequence near its N terminus. Other Glu-rich proteins interact with Ca^{2+} (Endo et al., 2004; Jo et al., 2004), and the Glu-rich region of *MtIRE* could have a

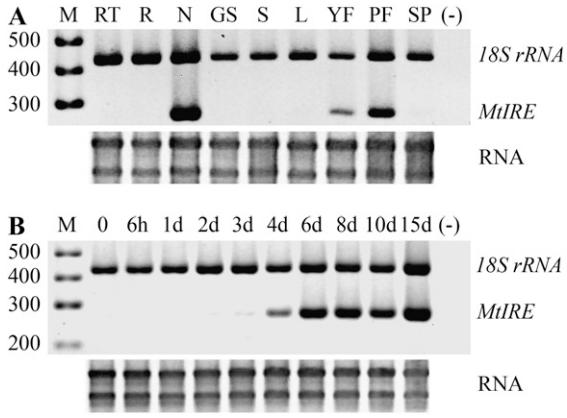

Figure 5. *MtIRE* gene expression in plant organs and during nodule development. A, Total RNA from plant organs was analyzed by semiquantitative RT-PCR in the presence of primers specific for *MtIRE* and for *rRNA* as positive control for RNA in the RT-PCR reaction. M, Markers whose sizes are on the left; RT, root tips; R, uninoculated roots; N, nodules; GS, germinated seeds; S, stems; L, leaves; YF, young unopened flowers; PF, pollinated flowers; SP, seed pods; (−), no RNA. Below the RT-PCR results is an ethidium bromide-stained agarose gel with 1 μg of total RNA from each sample used for the RT-PCR. B, Total RNA from nodulating roots was analyzed at the indicated times after inoculation of roots with *S. meliloti*. M, (−), as in A. Below the RT-PCR results is a gel with 1 μg of total RNA from each sample used for the RT-PCR.

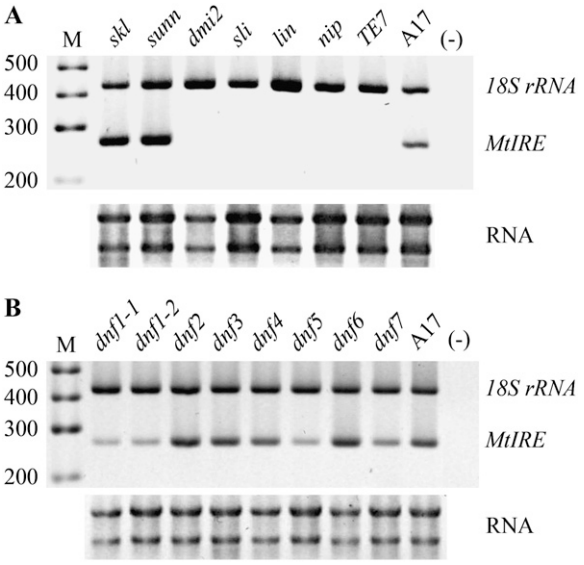

Figure 6. *MtIRE* gene expression in nodulation mutants. A, Total RNA from 10-dpi nodulated root systems of *skl*, *sunn*, *dmi2*, *sli*, *lin*, *nip*, *Mtsym1* (TE7), and wild-type (A17) plants was analyzed by semiquantitative RT-PCR in the presence of primers specific for *MtIRE* and for *rRNA* as positive control for RNA in the RT-PCR reaction. M, Markers whose sizes are on the left. Below the RT-PCR results is an ethidium-stained agarose gel with 1 μg of total RNA from each sample used for the RT-PCR. B, Total RNA from 10-dpi nodulated root systems of *dnf1-1*, *dnf1-2*, *dnf2*, *dnf3*, *dnf4*, *dnf5*, *dnf6*, *dnf7*, and wild-type (A17) plants was analyzed as in A. Below the RT-PCR results is a gel with 1 μg of total RNA from each sample used for the RT-PCR.

similar function. Although Ca^{2+} signaling has a well-documented role in the Nod factor signaling between rhizobia and legume roots (Levy et al., 2004; Mitra et al., 2004; Gleason et al., 2006; Tirichine et al., 2006), only a few studies have investigated the role of Ca^{2+} in intermediate and later stages of nodule development. In *Medicago*, the Ca^{2+}/calmodulin-dependent protein kinase DMI3 was recently shown to have a role in infection during rhizobial release from infection threads into host cells (Godfroy et al., 2006). In determinate soybean (*Glycine max*) nodules, two calmodulin genes were found to be expressed in the infection zone and proposed to be essential for Bradyrhizobium release into symbiosomes (Son et al., 2003). In *Medicago*, calmodulin transcripts are expressed in root nodules (Fedorova et al., 2002), and novel Ca^{2+}-binding proteins are found in the symbiosome space (Liu et al., 2006). Ca^{2+} has been found to modulate symbiosome membrane intake and efflux (Udvardi and Day, 1997).

Expression studies in developing nodules showed *MtIRE* expression is first detectable at 4 dpi in our growth conditions (Fig. 4). This time coincides with the time when symbiosomes are beginning to develop and is long before the onset of nitrogen fixation, at about 8 dpi in our conditions.

To correlate *MtIRE* expression with the phenotypes formed by nodulation mutants, it was necessary to define the mutated phenotypes in our growth conditions. Our findings show that at 10 dpi, *sli* nodules are blocked during invasion of the nodule primordia by rhizobia, different from the rare invaded nodules that are observed at a later time point (Haynes et al., 2004). The *dnf* mutant nodules are blocked after the rhizobia have invaded the nodules through infection threads and deposited rhizobia within host cells (Figs. 7 and 8). The extent of *dnf* mutant nodule development that we observed correlates well with previous plant and bacterial gene expression studies in the *dnf* mutants (Mitra and Long, 2004; Starker et al., 2006).

Comparing *MtIRE* expression in mutant nodulating root systems (Fig. 6) with phenotypes of the mutant nodules (Figs. 7 and 8) shows that *MtIRE* expression is associated only with nodules that are able to achieve successful invasion, release of rhizobia into infected cells, and some development of the resulting symbiosomes, i.e. the *dnf* mutants. *MtIRE* expression was not observed in the *sli* or *nip* mutants that have little to no rhizobial release from infection threads (Haynes et al., 2004; Veereshlingam et al., 2004). Nor was *MtIRE* expression found in *Mtsym1* (TE7) mutants that have rhizobial release from infection threads into symbiosomes but no obvious replication of rhizobia inside symbiosomes or elongation of rhizobia into bacteroids (Benaben et al., 1995). The finding that *MtIRE* expression is lower in *dnf1*, *dnf5*, and *dnf7* mutants may point to defects in these mutants that affect the physiology of infected nodule cell maturation in zone II.

In attempts to discern a function for *MtIRE*, we and others (S. Gantt, personal communication) have attempted *MtIRE* RNAi-induced gene silencing. The results have been inconsistent, with phenotypes that varied from root hair defects to defective nodulation to no detectable effect (data not shown). We have tried three different silencing constructs, with two chosen from *MtIRE* regions that are apparently unique to *MtIRE* and one from the putative Ser/Thr kinase domain. The lack of consistent results from any RNAi construct tested suggests possible functional redundancy in one or more of the other *Medicago IRE*-like genes. We note that another group has also reported similar issues with the RNAi technique (Liu et al., 2006).

Localization experiments using p*MtIRE-gusA* in transformed hairy root composite plants showed that *MtIRE* expression localizes to a band in the proximal part of zone II, the infection zone. To date, there are very few details about the biology or biochemistry of the symbiotic interaction in this nodule region. In this area of zone II, rhizobia are already released from infection threads, symbiosomes are starting to develop and the host cells are expanding, but the rhizobia are not capable of nitrogen fixation (Vasse et al., 1990). Localization of p*MtIRE-gusA* expression in *dnf1-2* and *dnf7* plants showed that while nodules from both mutants express p*MtIRE-gusA*, the *dnf1-2* plants appeared to halt nodule development after the zone where *MtIRE* is expressed, while the *dnf7* plants progressed further in nodulation. Thus, *MtIRE* may

be a good marker for the ability of nodules to progress to proximal zone II development.

MtIRE was found to be a single copy gene in *M. truncatula* and a member of the *IRE* clade of the AGC kinase family. The phylogenetic analysis suggests that *MtIRE* may be the ortholog of the *AtIRE* gene. We performed the phylogenetic analysis with the available, but partial, cDNA sequence for the three other *Medicago IRE* genes. When the full sequences of these cDNAs are available, it may turn out that one of them is a closer homolog to *AtIRE* than is *MtIRE*.

Our results demonstrated *MtIRE* expression in nodules and flowers (Fig. 3), similar to a number of other nodulins (Allison et al., 1993; Crespi et al., 1994;

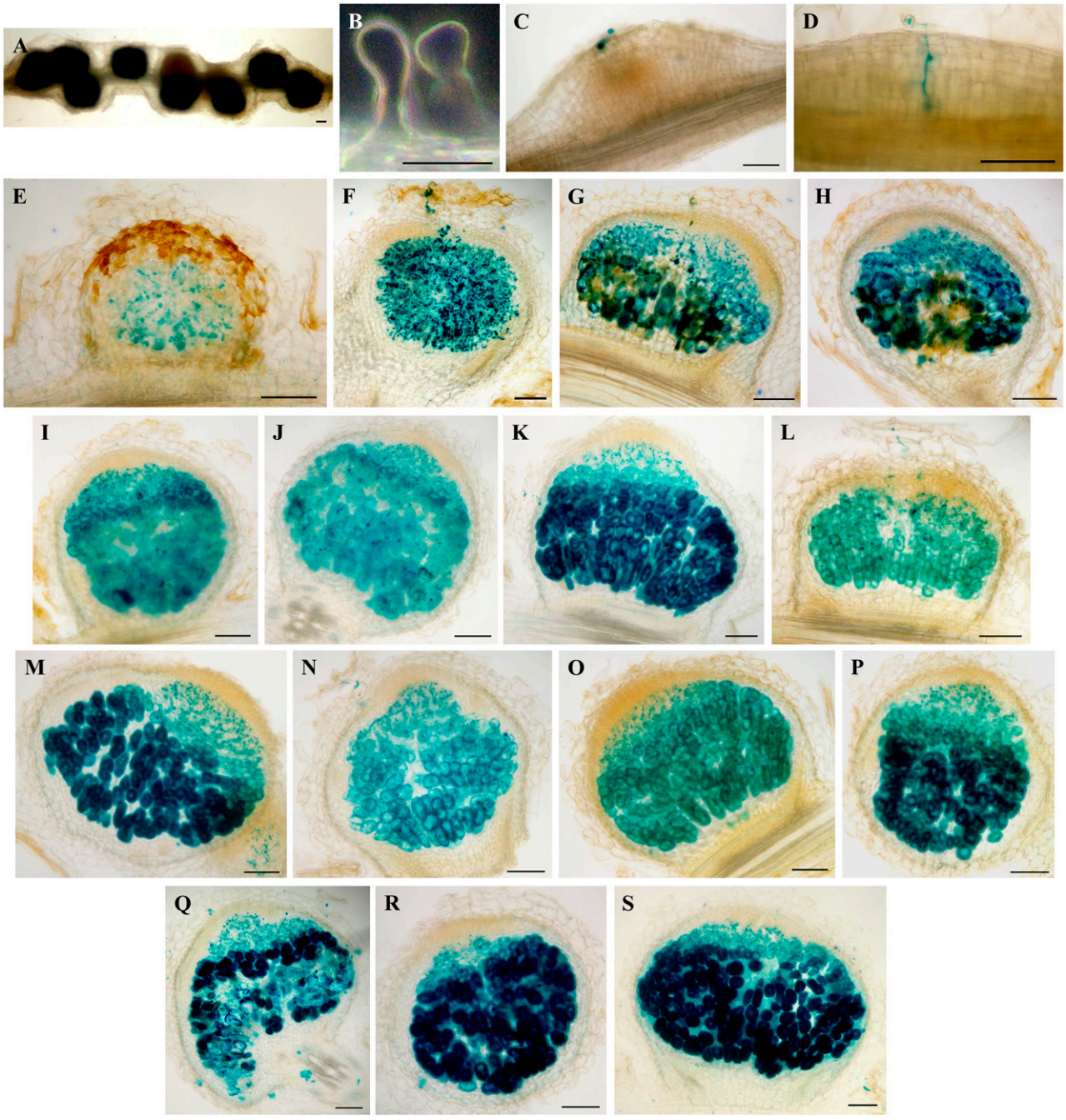

Figure 7. Phenotypes of nodules from nodulation mutants. Plant roots from the indicated mutants or wild type were grown in the presence of *S. meliloti*/pXLDG4 containing a constitutive *hemA*::*lacZ* construct and stained at 10 dpi with X-Gal. A, *skl*; B, *dmi2*; C, *lin*; D, *sli*; E, *nip*; F, *Mtsym1* (TE7); G, *dnf1-1*; H, *dnf1-2*; I, *dnf2*; J, *dnf3*; K, *dnf3* (similar to wild type); L, *dnf4*; M, *dnf4* (similar to wild type); N, *dnf5*; O, *dnf6*; P, *dnf6* (similar to wild type); Q, *dnf7*; R, *dnf7* (similar to wild type); S, A17 (wild type). Bars = 100 μm. A to D, Whole mounts; E to S, 50-μm sections.

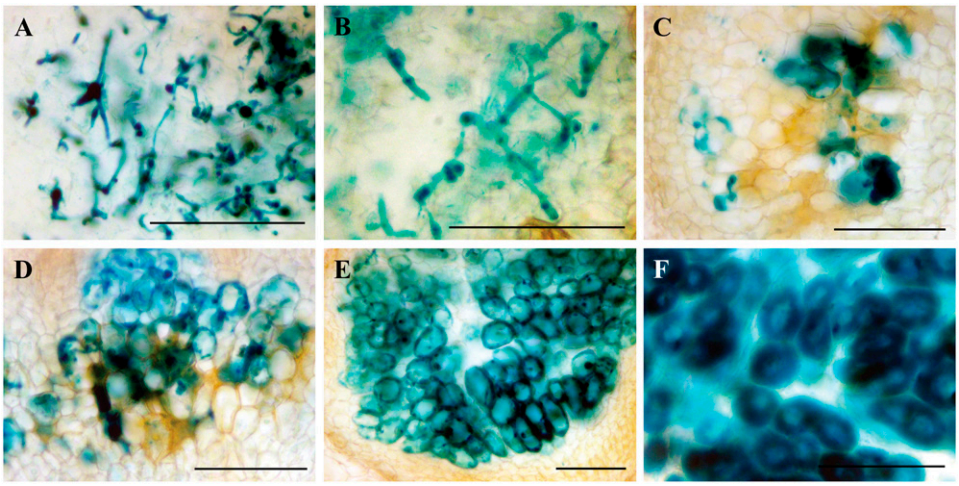

Figure 8. Higher magnification of phenotypes of nodulation mutants' nodules. Plant roots from the indicated mutants or wild type were grown in the presence of *S. meliloti*/pXLDG4 containing a constitutive *hemA*::*lacZ* construct and stained at 10 dpi with X-Gal. A, *Mtsym1* (TE7); B, *nip*; C, *dnf1-1*; D, *dnf1-2*; E, *dnf5*; F, A17 (wild type). Bars = 100 μm. All are 50-μm sections.

Zucchero et al., 2001; Rodriguez-Llorente et al., 2004). The *MtIRE* expression pattern has diverged from the orthologous *AtIRE* gene that is expressed in every organ of the wild-type plant, with higher expression in roots (Oyama et al., 2002), suggesting that *MtIRE* has been recruited to nodule development from another role. Several previous studies have highlighted recruitment of genes from other plant programs to symbiotic processes as an evolutionary mechanism of the nitrogen-fixing symbiosis (Szczyglowski and Amyot, 2003; Rodriguez-Llorente et al., 2004; Liu et al., 2006). These include the *ENOD* genes, genes that transduce signals from both the arbuscular mycorrhizal and rhizobial symbioses, genes that control nodule number, and genes for leghemoglobin, all of which appear to have been derived from other functions in plant ancestors that gave rise to legumes. *AtIRE* regulates the duration of root hair cell expansion in Arabidopsis (Oyama et al., 2002). Our data show that the *MtIRE* gene has unique expression during nodule development in zone II, where the expansion and development of host cells and symbiosomes take place. Because of this, we propose that the recruited *MtIRE* gene has a role in these processes and, because it apparently encodes an AGC kinase, we propose that this role is in signal transduction.

MATERIALS AND METHODS

Plants, Growth Conditions, and Rhizobial Strain

Medicago truncatula A17 (wild type) and nodulation mutants were grown in aeroponic chambers, starved for nitrogen for 5 d, and inoculated with *Sinorhizobium meliloti* harboring pXLDG4 (Boivin et al., 1990; Penmetsa and Cook, 1997), as described previously (Veereshlingam et al., 2004).

Cloning *MtIRE*

RT-PCR was used to clone *MtIRE* from total RNA extracted from *M. truncatula* root nodules using standard protocols (Ausubel et al., 1988). RT primers and reverse primers for PCR had the following sequences: 2371r, 5′-GTATTTCGGGTGCCAAATAATC; and 3254r, 5′-GGGTGAAAGACATTACAGTGTCTG. Forward PCR primers were: 40f, 5′-CCATGTCTTCCAACCCTCC; 130f, 5′-GGAGTTAGGCCTTTTCCAGTCT; and 2005f, 5′-GGAGTACTTAAATGGTGGAGATCTCT. RNA ligase mediated-RACE for both the 5′ and 3′ ends of *MtIRE* was performed using the FirstChoice RNA ligase mediated-RACE kit according to the manufacturer's instructions (Ambion). DNA sequencing of the *MtIRE* cDNA was performed in the University of North Texas DNA sequencing lab using custom primers. Both strands were sequenced to completion.

Sequence and Phylogenetic Analysis

ExPASy (www.expasy.org/tools/scanprosite; Gattiker et al., 2002), BLAST (www.ncbi.nlm.nih.gov/BLAST/; Altschul et al., 1990), and BioEdit (Hall, 1999) tools were used to analyze the deduced *MtIRE* protein. Phylogenetic analysis using ClustalW (Thompson et al., 1994) and the neighbor-joining method were done at pir.georgetown.edu/pirwww/search/multaln.html.

Gene Expression by Semiquantative RT-PCR

The *MtIRE* primers were designed to span introns: MtIRE F, 5′-CATCCATAAAGACCTAGGGGAAAAAGTTC; and MtIRE R, 5′-CTCCATGATTTCCTGCCCAAAGGC. The 18S rRNA F is 5′-CCAGGTCCAGACATAGTAAG and the 18S rRNA R is 5′-GTACAAAGGGCAGGGACGTA. Two micrograms of total RNA, extracted as described previously (Veereshlingam et al., 2004), was reverse transcribed using M-MuLV reverse transcriptase in a 25-μL reaction containing 1× RT buffer (NE Biolabs), 1 mM dNTPs, 100 nM MtIRE R primer, and 50 nM 18S rRNA R primer at 37°C for 1 h. A total of 5 μL of the RT was amplified in a 50-μL PCR reaction consisting of 1× Thermopol buffer (NE Biolabs), 200 μM dNTPs, 250 nM MtIRE primers, and 50 nM 18S rRNA primers. After 4 min at 94°C, 30 or 35 cycles of PCR were run using 94°C 30 s, 61°C for 25 s, and 72°C for 20 s.

Histochemical Staining of Wild Type and Nodulation Mutants

Nodules elicited with *S. meliloti/pXLDG4* containing the constitutive *hemA*::*lacZ* gene were stained with X-Gal, as described previously (Veereshlingam et al., 2004), by using standard methods (Boivin et al., 1990). The buffer used in our protocols was 80 mM PIPES, pH 7.2, instead of cacodylate. For sectioning, nodules were embedded in 5% low-melting point agarose and 50-μm-thick sections were obtained with a 1000 Plus Vibratome (Vibratome). Sections were observed with an Olympus BX50 microscope using bright field or dark field (for *dmi2* roots). Digital micrographs were processed using Adobe Photoshop.

MtIRE Promoter-*GUS* Reporter Construct and *M. truncatula* Root Transformation

pRD022 was created by subcloning the *Sph*I fragment from pCAMBIA2301 (Hajdukiewicz et al., 1994) containing the cauliflower mosaic virus promoter-GUS coding region into pUC18. A large region upstream (3,458 bp) of the *MtIRE*

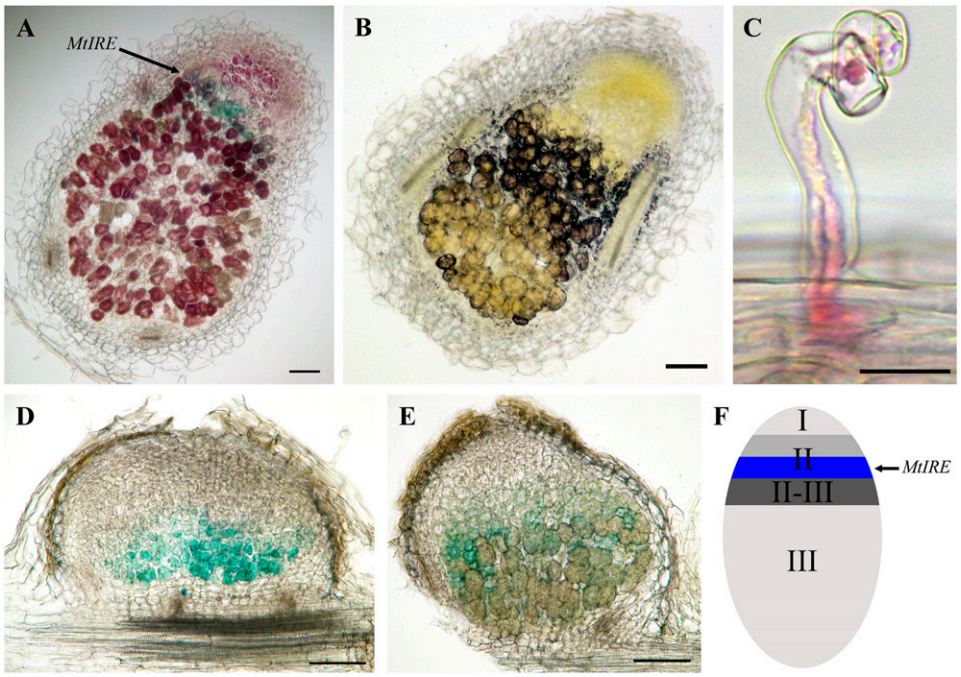

Figure 9. Localization of p*MtIRE-gusA* expression in wild-type and *dnf1-2* and *dnf7* mutants. Composite *M. truncatula* plants with transgenic roots were grown in the presence of *S. meliloti* containing a constitutive *lacZ* gene. A, Double staining for *gusA* with X-gluc (blue), for the localization of *MtIRE* promoter activity, and *lacZ* with Red-Gal (red), for the rhizobia localization. The arrow points to the X-gluc staining. Bar = 100 μm. B, Staining with iodide reveals the position of interzone II-III. Bar = 100 μm. C, Root hair with an infection thread stained with X-gluc and Red-Gal shows rhizobia staining but no p*MtIRE-gusA* staining. Bar = 20 μm. D, *dnf1-2* nodule stained with X-gluc only shows p*MtIRE-gusA* staining in proximal part of nodule. Bar = 100 μm. E. *dnf7* nodule stained with X-gluc only shows p*MtIRE-gusA* staining in middle of nodule. Bar = 100 μm. F, Interpretative diagram of A and B showing the position of *MtIRE* expression in the proximal region of the invasion zone, zone II.

gene was amplified from the mth2-13b8 BAC clone (obtained from the Clemson Stock Center, www.genome.clemson.edu). The forward primer MtIREp F has an *Eco*RI site at its 5′ end, 5′-TGGAATTCCTGCATGGCGCGAGCAAAATGT, and the reverse primer MtIREp R has an *Nco*I site at its 5′ end, 5′-ACCATGGTGAGAGATGAAAGGAAGAGAG. After PCR amplification (94°C 2 min, followed by 35 cycles of 94°C 30 s, 60°C 30 s, 72°C 3 min), the resulting product was digested with *Eco*RI and *Nco*I and ligated to *Eco*RI, *Nco*I-digested pRD022, replacing the cauliflower mosaic virus promoter with the *MtIRE* promoter. This plasmid was then digested with *Eco*RI and *Bst*EII and ligated with *Eco*RI, *Bst*EII-digested pCAMBIA2301 to create pCIP005. pCIP005 was transformed into *Agrobacterium rhizogenes* strain ARqua1 (Quandt et al., 1993) using the freeze-thaw method (Hofgen and Willmitzer, 1988). *M. truncatula* roots were transformed *A. rhizogenes* strains (Boisson-Dernier et al., 2001) containing pCIP005 or a positive control containing the p*ENOD11-gusA* construct (Journet et al., 2001).

Histochemical Staining of Root Nodules on Transformed Roots

GUS activity in whole roots was detected after fixation in 0.3% paraformaldehyde and infiltration with X-gluc, as described by Jefferson (Jefferson et al., 1987). Composite plants transformed with the p*ENOD11-gusA* construct served as control and yielded results similar to published ones (Boisson-Dernier et al., 2001; Journet et al., 2001). For dual staining with Red-Gal, roots were stained first with X-gluc, then the X-gluc was replaced with 1 mM Red-Gal (6-chloro-3-indoyl-β-D-galactoside; Research Organics). Staining nodules for starch was done as described (Vasse et al., 1990), except that 0.1 M PIPES, pH 7.2, was used as the buffer. Sectioning, visualization, and processing of images were done as described above.

All experiments were done in at least duplicate.

Sequence data for the genes discussed in this article can be found in the GenBank databases under the following accession numbers: *MtIRE*, AAX11214; *AtIRE*, NP_201037; *AtIRE H1*, NP_188412; *AtIRE2*, BAB02708; *AtIRE3*, NP_001031155; *AtIRE4*, NP_175130; *OsIRE*, ABA99908; *OsIRE1*, XP_469518; *OsIRE2*, ABF98517; *OsIRE3*, ABF98518; *OsIRE4*, AK122108; *LeIRE*, BT013855; *AtPDK1_1*, NP_974730; *AtPDK1_2*, ABF57283; *AtS6K_2*, NP_850543; *AtS6K_1*, NP_187485; *AtNDR1*, NP_849380; *AtNDR2*, NP_171888; *AtNDR3*, NP_188973; *AtNDR4*, NP_565453; *AtNDR5*, NP_179637; *AtNDR6*, NP_195034; *AtNDR7*, NP_174352; *AtNDR8*, NP_568221; *AtAGC1_1*, NP_200402; *AtAGC1_2*, NP_194391; *AtAGC1_3*, NP_850426; *AtAGC1_4*, NP_198819; *AtAGC1_5*, AAV85687; *AtAGC1_6*, NP_173094; *AtAGC1_7*, NP_178045; *AtAGC1_8*, NP_195984; *AtAGC1_9*, NP_181176; *AtAGC1_10*, NP_180238; *AtAGC1_11*, NP_188054; *AtAGC1_12*, NP_190047; *AtPK3*, NP_175774; *AtPK5*, NP_199586; *AtPK7*, AAQ65194; *AtKIPK*, NP_850687; *AtPID*, NP_181012; *AtAGC2_1* (*OXI1*), NP_189162; *AtAGC2_2*, NP_193036; *AtAGC2_3*, NP_564584; *AtAGC2_4*, NP_188719; *AtPHOT1*, NP_190164; and *AtPHOT2*, NP_568874.

ACKNOWLEDGMENTS

We thank several *Medicago* researchers for nodulation mutant seeds: Drs. Douglas Cook, Thierry Huguet, Sharon Long, Giles Oldroyd, Varma Penmetsa, Colby Starker, and Kate VandenBosch. We thank Heath Wessler for help with DNA sequencing, and Etienne Journet and David Barker for providing the p*ENOD11-gusA* construct used as a control in root transformation and X-gluc staining experiments (not shown). We thank Ed Braun for helpful discussions about the phylogenetic analysis.

Received November 1, 2006; accepted January 1, 2007; published January 19, 2007.

LITERATURE CITED

Allison LA, Kiss GB, Bauer P, Poiret M, Pierre M, Savoure A, Kondorosi E, Kondorosi A (1993) Identification of two alfalfa early nodulin genes with homology to members of the pea *Enod12* family. Plant Mol Biol **21:** 375–380

Altschul SF, Gish W, Miller W, Meyers EW, Lipman DJ (1990) Basic local alignment search tool. J Mol Biol **215:** 403–410

Anthony RG, Henriques R, Helfer A, Meszaros T, Rios G, Testerink C, Munnik T, Deak M, Koncz C, Bogre L (2004) A protein kinase target of a PDK1 signalling pathway is involved in root hair growth in *Arabidopsis*. EMBO J **23:** 572–581

Anthony RG, Khan S, Costa J, Pais MS, Bogre L (2006) The *Arabidopsis* protein kinase PTI1-2 is activated by convergent phosphatidic acid and oxidative stress signaling pathways downstream of PDK1 and OXI1. J Biol Chem **281:** 37536–37546

Ardourel M, Demont N, Debelle F, Maillet F, de Billy F, Prome JC, Denarie J, Truchet G (1994) *Rhizobium meliloti* lipooligosaccharide nodulation factors: different structural requirements for bacterial entry into target root hair cells and induction of plant symbiotic developmental responses. Plant Cell **6:** 1357–1374

Ausubel FM, Brent R, Kingston RE, Moore DD, Seidman JG, Smith JA, Struhl K (1988) Current Protocols in Molecular Biology. Wiley Interscience, New York

Benaben V, Duc G, Lefebvre V, Huguet T (1995) TE7, an inefficient symbiotic mutant of *Medicago truncatula* Gaertn. cv Jemalong. Plant Physiol **107:** 53–62

Bogre L, Okresz L, Henriques R, Anthony RG (2003) Growth signalling pathways in *Arabidopsis* and the AGC protein kinases. Trends Plant Sci **8:** 424–431

Bohm S, Frishman D, Mewes HW (1997) Variations of the C_2H_2 zinc finger motif in the yeast genome and classification of yeast Zn finger proteins. Nucleic Acids Res **25:** 2464–2469

Boisson-Dernier A, Chabaud M, Garcia F, Becard G, Rosenberg C, Barker DG (2001) *Agrobacterium rhizogenes*-transformed roots of *Medicago truncatula* for the study of nitrogen-fixing and endomycorrhizal symbiotic associations. Mol Plant Microbe Interact **14:** 695–700

Boivin C, Camut S, Malpica CA, Truchet G, Rosenberg C (1990) *Rhizobium meliloti* genes encoding catabolism of trigonelline are induced under symbiotic conditions. Plant Cell **2:** 1157–1170

Brewin NJ (1991) Development of the legume root nodule. Annu Rev Cell Biol **7:** 191–226

Brewin NJ (2004) Plant cell wall remodelling in the Rhizobium-legume symbiosis. CRC Crit Rev Plant Sci **23:** 293–316

Briggs WR, Christie JM (2002) Phototropins 1 and 2: versatile plant blue-light receptors. Trends Plant Sci **7:** 204–210

Catoira R, Galera C, de Billy F, Penmetsa RV, Journet EP, Maillet F, Rosenberg C, Cook D, Gough C, Denarie J (2000) Four genes of *Medicago truncatula* controlling components of a Nod factor transduction pathway. Plant Cell **12:** 1647–1666

Christensen SK, Dagenais N, Chory J, Weigel D (2000) Regulation of auxin response by the protein kinase PINOID. Cell **100:** 469–478

Crespi MD, Jurkevitch E, Poiret M, d'Aubenton-Carafa Y, Petrovics G, Kondorosi E, Kondorosi A (1994) *enod40*, a gene expressed during nodule organogenesis, codes for a non-translatable RNA involved in plant growth. EMBO J **13:** 5099–5112

Devarenne TP, Ekengren SK, Pedley KF, Martin GB (2006) Adi3 is a Pdk1-interacting AGC kinase that negatively regulates plant cell death. EMBO J **25:** 255–265

El Yahyaoui F, Kuster H, Ben Amor B, Hohnjec N, Puhler A, Becker A, Gouzy J, Vernie T, Gough C, Niebel A, et al (2004) Expression profiling in *Medicago truncatula* identifies more than 750 genes differentially expressed during nodulation, including many potential regulators of the symbiotic program. Plant Physiol **136:** 3159–3176

Endo H, Takagi Y, Ozaki N, Kogure T, Watanabe T (2004) A crustacean Ca2+-binding protein with a glutamate-rich sequence promotes CaCO3 crystallization. Biochem J **384:** 159–167

Fedorova M, van de Mortel J, Matsumoto PA, Cho J, Town CD, VandenBosch KA, Gantt JS, Vance CP (2002) Genome-wide identification of nodule-specific transcripts in the model legume *Medicago truncatula*. Plant Physiol **130:** 519–537

Gage DJ (2004) Infection and invasion of roots by symbiotic, nitrogen-fixing rhizobia during nodulation of temperate legumes. Microbiol Mol Biol Rev **68:** 280–300

Gage DJ, Margolin W (2000) Hanging by a thread: invasion of legume plants by rhizobia. Curr Opin Microbiol **3:** 613–617

Gattiker A, Gasteiger E, Bairoch A (2002) ScanProsite: a reference implementation of a PROSITE scanning tool. Appl Bioinformatics **1:** 107–108

Gleason C, Chaudhuri S, Yang T, Munoz A, Poovaiah BW, Oldroyd GED (2006) Nodulation independent of rhizobia induced by a calcium-activated kinase lacking autoinhibition. Nature **441:** 1149–1152

Godfroy O, Debellé F, Timmers T, Rosenberg C (2006) A rice calcium- and calmodulin-dependent protein kinase restores nodulation to a legume mutant. Mol Plant Microbe Interact **19:** 495–501

Hajdukiewicz P, Svab Z, Maliga P (1994) The small, versatile pPZP family of *Agrobacterium* binary vectors for plant transformation. Plant Mol Biol **25:** 989–994

Hall TA (1999) BioEdit: a user-friendly biological sequence alignment editor and analysis program for Windows 95/98/NT. Nucleic Acids Symp Ser **41:** 95–98

Hanks SK, Hunter T (1995) The eukaryotic protein kinase superfamily: kinase (catalytic) domain structure and classification. FASEB J **9:** 576–596

Haynes JG, Cyzmmek KJ, Carlson CA, Veereshlingam H, Dickstein R, Sherrier DJ (2004) A novel method for rapid analysis of legume root nodule development using confocal microscopy. New Phytol **163:** 661–668

Hofgen R, Willmitzer L (1988) Storage of competent cells for *Agrobacterium* transformation. Nucleic Acids Res **16:** 9877

Huala E, Oeller PW, Liscum E, Han I-S, Larsen E, Briggs WR (1997) *Arabidopsis* NPH1: a protein kinase with a putative redox-sensing domain. Science **278:** 2120–2123

Jefferson R, Kavanagh T, Bevan M (1987) GUS fusions: β-glucuronidase as a sensitive and versatile gene fusion marker in higher plants. EMBO J **6:** 3901–3907

Jo D-G, Jun J-I, Chang J-W, Hong Y-M, Song S, Cho D-H, Shim SM, Lee H-J, Cho C, Kim DH, et al (2004) Calcium binding of ARC mediates regulation of caspase 8 and cell death. Mol Cell Biol **24:** 9763–9770

Journet EP, El-Gachtouli N, Vernoud B, de Billy F, Pichon M, Dedieu A, Arnould C, Morandi D, Barker DG, Gianinazzi-Pearson V (2001) *Medicago truncatula ENOD11*: a novel RPRP-encoding early nodulin gene expressed during mycorrhization in arbuscule-containing cells. Mol Plant Microbe Interact **14:** 737–748

Kalderon D, Richardson WD, Markham AF, Smith AE (1984) Sequence requirements for nuclear localization of simian virus 40 large-T antigen. Nature **311:** 33–38

Kijne JW (1992) The *Rhizobium* infection process. *In* G Stacey, HJ Evans, RH Burris, eds, Biological Nitrogen Fixation. Chapman and Hall, London, pp 349–398

Kuppusamy KT, Endre G, Prabhu R, Penmetsa RV, Veereshlingam H, Cook DR, Dickstein R, Vandenbosch KA (2004) *LIN*, a *Medicago truncatula* gene required for nodule differentiation and persistence of rhizobial infections. Plant Physiol **136:** 3682–3691

Levy J, Bres C, Geurts R, Chalhoub B, Kulikova O, Duc G, Journet E-P, Ane J-M, Lauber E, Bisseling T, et al (2004) A putative Ca2+ and calmodulin-dependent protein kinase required for bacterial and fungal symbioses. Science **303:** 1361–1364

Limpens E, Franken C, Smit P, Willemse J, Bisseling T, Geurts R (2003) LysM domain receptor kinases regulating rhizobial Nod factor-induced infection. Science **302:** 630–633

Liu J, Miller SS, Graham M, Bucciarelli B, Catalano C, Sherrier DJ, Samac DA, Ivashuta S, Fedorova M, Matsumoto P, et al (2006) Recruitment of novel calcium binding proteins for root nodule symbiosis in *Medicago truncatula*. Plant Physiol **141:** 167–177

Lohar DP, Sharopova N, Endre G, Penuela S, Samac D, Town C, Silverstein KAT, VandenBosch KA (2006) Transcript analysis of early nodulation events in *Medicago truncatula*. Plant Physiol **140:** 221–234

Mitra RM, Gleason CA, Edwards A, Hadfield J, Downie JA, Oldroyd GED, Long SR (2004) A Ca2+/calmodulin-dependent protein kinase required for symbiotic nodule development: gene identification by transcript-based cloning. Proc Natl Acad Sci USA **101:** 4701–4705

Mitra RM, Long SR (2004) Plant and bacterial symbiotic mutants define three transcriptionally distinct stages in the development of the *Medicago truncatula*/*Sinorhizobium meliloti* symbiosis. Plant Physiol **134:** 595–604

Mora A, Komander D, van Aalten DMF, Alessi DR (2004) PDK1, the master regulator of AGC kinase signal transduction. Semin Cell Dev Biol **15:** 161–170

Oyama T, Shimura Y, Okada K (2002) The *IRE* gene encodes a protein kinase homologue and modulates root hair growth in *Arabidopsis*. Plant J **30:** 289–299

Penmetsa RV, Cook DR (1997) A legume ethylene-insensitive mutant hyperinfected by its rhizobial symbiont. Science **275:** 527–530

Penmetsa RV, Frugoli JA, Smith LS, Long SR, Cook DR (2003) Dual genetic pathways controlling nodule number in *Medicago truncatula*. Plant Physiol **131:** 998–1008

Quandt HJ, Puhler A, Broer I (1993) Transgenic root nodules of *Vicia hirsuta*: a fast and efficient system for the study of gene expression in indeterminate-type nodules. Mol Plant Microbe Interact **6:** 699–706

Rentel MC, Lecourieux D, Ouaked F, Usher SL, Peterson L, Okamoto H, Knight H, Peck SC, Grierson CS, Hirt H, et al (2004) OXI1 kinase is necessary for oxidative burst-mediated signalling in *Arabidopsis*. Nature **427:** 858–861

Robbins J, Dilworth SM, Laskey RA, Dingwall C (1991) Two interdependent basic domains in nucleoplasmin nuclear targeting sequence: identification of a class of bipartite nuclear targeting sequence. Cell **64:** 615–623

Rodriguez-Llorente I, Perez-Hormaeche J, El Mounadi K, Dary M, Caviedes MA, Cosson V, Kondorosi A, Ratet P, Palomares AJ (2004) From pollen tubes to infection threads: recruitment of *Medicago* floral pectic genes for symbiosis. Plant J **39:** 587–598

Sanderson MJ, Thorne JL, Wikstron N, Bremer K (2004) Molecular evidence on plant divergence times. Am J Bot **91:** 1656–1665

Schiefelbein JW (2000) Constructing a plant cell. The genetic control of root hair development. Plant Physiol **124:** 1525–1531

Son O, Yang H-S, Lee H-J, Lee M-Y, Shin K-H, Jeon S-L, Lee M-S, Choi S-Y, Chun J-Y, Kim H, et al (2003) Expression of srab7 and SCaM genes required for endocytosis of Rhizobium in root nodules. Plant Sci **165:** 1239–1244

Starker CG, Parra-Colmenares AL, Smith L, Mitra RM, Long SR (2006) Nitrogen fixation mutants of *Medicago truncatula* fail to support plant and bacterial symbiotic gene expression. Plant Physiol **140:** 671–680

Szczyglowski K, Amyot L (2003) Symbiosis, inventiveness by recruitment? Plant Physiol **131:** 935–940

Takemiya A, Inoue S-i, Doi M, Kinoshita T, Shimazaki K-i (2005) Phototropins promote plant growth in response to blue light in low light environments. Plant Cell **17:** 1120–1127

Tamaskovic R, Bichsel SJ, Hemmings BA (2003) NDR family of AGC kinases: essential regulators of the cell cycle and morphogenesis. FEBS Lett **546:** 73–80

Thompson JD, Higgins DG, Gibson TJ (1994) CLUSTAL W: improving the sensitivity of progressive multiple sequence alignment through sequence weighting, positions-specific gap penalties and weight matrix choice. Nucleic Acids Res **22:** 4673–4680

Tirichine L, Imaizumi-Anraku H, Yoshida S, Murakami Y, Madsen LH, Miwa H, Nakagawa T, Sandal N, Albrektsen AS, Kawaguchi M, et al (2006) Deregulation of a Ca^{2+}/calmodulin-dependent kinase leads to spontaneous nodule development. Nature **441:** 1153–1156

Udvardi MK, Day DA (1997) Metabolite transport across symbiotic membranes of legume nodules. Annu Rev Plant Physiol Plant Mol Biol **48:** 493–523

Vasse J, de Billy F, Camut S, Truchet G (1990) Correlation between ultrastructural differentiation of bacteroids and nitrogen fixation in alfalfa nodules. J Bacteriol **172:** 4295–4306

Veereshlingam H, Haynes JG, Sherrier DJ, Penmetsa RV, Cook DR, Dickstein R (2004) *nip*, a symbiotic *Medicago truncatula* mutant that forms root nodules with aberrant infection threads and plant defense-like response. Plant Physiol **136:** 3692–3702

Young ND, Cannon SB, Sato S, Kim D, Cook DR, Town CD, Roe BA, Tabata S (2005) Sequencing the genespaces of *Medicago truncatula* and *Lotus japonicus*. Plant Physiol **137:** 1174–1181

Zegzouti H, Anthony RG, Jahchan N, Bogre L, Christensen SK (2006) Phosphorylation and activation of *PINOID* by the phospholipid signaling kinase 3-phosphoinositide-dependent protein kinase 1 (PDK1) in *Arabidopsis*. Proc Natl Acad Sci USA **103:** 6404–6409

Zegzouti H, Li W, Lorenz TC, Xie M, Payne CT, Smith K, Glenny S, Payne GS, Christensen SK (2007) Structural and functional insights into the regulation of *Arabidopsis* AGC VIIIa kinases. J Biol Chem **281:** 35520–35530

Zucchero JC, Caspi M, Dunn K (2001) *ngl9*, a third MADS box gene expressed in alfalfa root nodules. Mol Plant Microbe Interact **14:** 1463–1467

CORRECTIONS

Vol. 144: 682–694, 2007

Pislariu C. and Dickstein R. An *IRE*-Like AGC Kinase Gene, *MtIRE*, Has Unique Expression in the Invasion Zone of Developing Root Nodules in *Medicago truncatula.*

On Page 687, the first full sentence in the right column should read as follows: ''Plants were inoculated with rhizobia carrying a constitutive *lacZ* gene, and nodulated roots were harvested at 15 dpi.''

www.plantphysiol.org/cgi/doi/10.1104/pp.104.900231

Vol. 144: 1240–1246, 2007

Weiss D. and Ori N. Mechanisms of Cross Talk between Gibberellin and Other Hormones.

In Figure 3 of this *Update*, the inhibition bar from Aux/IAA to DELLA should be an arrow. The corrected figure is below.

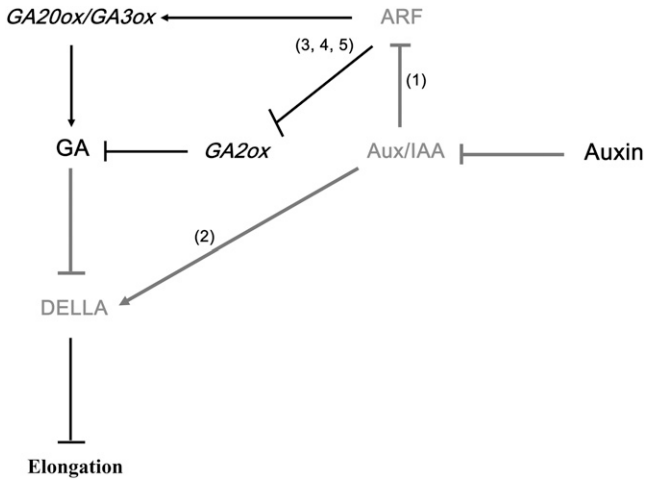

www.plantphysiol.org/cgi/doi/10.1104/pp.104.900232